Food Chemistry 434 (2024) 137450

Contents lists available at ScienceDirect

Food Chemistry

journal homepage: www.elsevier.com/locate/foodchem

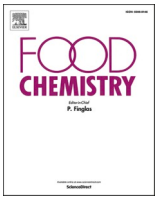

Effect of variation in basic emulsion structure and polysaccharide content on the physicochemical properties and structure of composite-based emulsion gels as cube fat mimetics

Yuqing Ren [a], Lai Wei [a], Jun Hao Yoong [b], Zhiyue Miao [b], He Li [a,*], Jinnuo Cao [c], Xinqi Liu [a,*]

[a] Key Laboratory of Geriatric Nutrition and Health (Beijing Technology and Business University), Ministry of Education, Beijing, China
[b] Palm Oil Research and Technical Service Institute of Malaysian Palm Oil Board, Shanghai, China
[c] Puluting (Hebei) Protein Biotechnology Research Limited Company, Handan, China

ARTICLE INFO

Keywords:
Cube fat substitute
Emulsion gel
Double emulsion gel
Protein-polysaccharide composite based
Plant-based fat mimetic

ABSTRACT

This study aimed to reveal the effect of different basic emulsion structures (W/O/W and O/W) and polysaccharide additions on protein-polysaccharide composite-based emulsion gels utilizing soybean protein isolate, palm oil and konjac glucomannan. The results of texture profile, rheological tests, microstructure observations, and oral tribology showed that basic emulsion structures and konjac glucomannan addition had significant effect on the emulsion gels' properties, while the impact of konjac glucomannan addition was stronger. W/O/W double emulsion gels (DEG) exhibited lower oral friction coefficients and obtained higher scores for oiliness and juiciness during the sensory evaluation. However, O/W single emulsion gels (SEG) displayed a firmer texture and higher chewiness, a 29.62% and 49.57% increase compared to the DEG at 7% konjac glucomannan addition on the hardness and chewiness respectively. It has demonstrated the emulsion gels' potential as cube fat mimetics and feasibility of adjusting their properties by changing the basic emulsion structure.

1. Introduction

The growing global population places an increasing demand on animal meat products, which is expected to rise significantly since the world population is projected to reach 11.2 billion by 2100(Lang, et al., 2021). As a major source of animal meat, livestock farming can lead to serious global problems. Furthermore, animal welfare issues are attracting increasing attention. More importantly, the excessive consumption of animal meat products poses a potential health risk to consumers, with the richness of saturated fatty acids and cholesterol being associated with a higher incidence of cardiovascular disease. Therefore, considering global environmental issues, sustainable development, and public health concerns, reducing dependence on meat products, decreasing the fat content in these products, and developing plant-based fat mimetics to replace real animal fats are important strategies for advancing food science and engineering.

To improve the nutritional attributes of meat products or fat substitutes, vegetable oils rich in unsaturated fatty acids are often used as substitutes for animal fats. However, collagen provides animal fats with plasticity and elasticity and can form fat particles after grinding or chopping, which are crucial textural and sensory components of meat products (Jimenez-Colmenero, et al., 2015), providing visible fat chunks and a unique mouthfeel. Therefore, simply replacing animal fats with liquid vegetable oils that lack the elasticity and plasticity of animal fats decreases the sensory quality of meat products, failing to meet the demands of consumers. Structured oils are considered effective in solving this problem (Herrero & Ruiz-Capillas, 2021), allowing liquid oils to acquire solid properties closer to real fats.

Emulsion gel is a soft solid material. As an emulsion with solid mechanical properties, the continuous phase forms a gel network in which the droplets can be dispersed. Protein-based oil-in-water emulsions typically form gel networks in the aqueous phase via acid-induction, thermal-induction, enzyme-induction, or polysaccharide addition (Dickinson, Radford, & Golding, 2003), during which the oil droplets are immobilized as dispersed phases to provide the entire system with solid properties. Emulsion gels with a soft texture are effective for structuring oils and have attracted significant attention due to their fat-like physical behavior in meat products, prompting many related studies involving

* Corresponding authors.
E-mail addresses: ryq512@163.com (Y. Ren), weilai00109@163.com (L. Wei), jhyoong@mpob.com.cn (J. Hao Yoong), miaozhiyue@mpob.com.cn (Z. Miao), lihe@btbu.edu.cn (H. Li), jinnuocao@163.com (J. Cao), liuxinqi@btbu.edu.cn (X. Liu).

https://doi.org/10.1016/j.foodchem.2023.137450
Received 25 May 2023; Received in revised form 2 September 2023; Accepted 8 September 2023
Available online 14 September 2023

utilizing these gels as fat substitutes (Heck, et al., 2019; Nacak, Ozturk-Kerimoglu, Yildiz, Cagindi, & Serdaroglu, 2021). However, most emulsion gels display are typically added to emulsified meat products or meat batters to replace fats due to their high viscosity and soft texture and challenging to form into cube fat substitutes. Some studies (Chen, Zhao, Li, Liu, & Kong, 2021; Huang, et al., 2022; Huang et al., 2022) have produced three-dimensional (3D) cube fat by adding polysaccharides to provide single emulsion gels (SEG) with a certain degree of hardness and high gel strength, increasing their appearance and textural similarity to real fat particles.

In addition to traditional oil-in-water and water-in-oil emulsions that can be used as the base for emulsion gels, unique emulsions, such as double emulsions, are also available. Double emulsions have multi-compartment structures in which oil-in-water and water-in-oil states coexist, presenting potential advantages over traditional oil-in-water single emulsions for encapsulating, delivering, and protecting active hydrophilic compounds. In addition, although several studies (Eisinaite, Juraite, Schroen, & Leskauskaite, 2017; Kumar & Kumar, 2020) have used double emulsions as fat substitutes to develop low-fat meat products, minimal research is available regarding double emulsion gels (DEG). Studies have shown (Chen, et al., 2022) that gelation of the external aqueous phase provides the double emulsion with elastic gel properties and improves its general and encapsulation stability. In terms of fat substitution, Freire et al. (Freire, et al., 2017) added gelatin and transglutaminase to the external aqueous phase of a double emulsion to create a pork patty fat substitute. Although complete fat substitution decreased the product acceptability, the significant fat content reduction confirmed the feasibility of using DEGs to develop fat mimetics. On the basis of previous studies, we hypothesized that the addition of polysaccharides to the external aqueous phase of the double emulsion could lead to the formation of DEGs that could be used as cube fat mimics. And due to the special multi-compartmental structure of double emulsions different from single emulsions, we speculated that DEGs may exhibit different properties from SEGs, such as different hardness, mouthfeel, or oral tribological behaviors, provided that the main ingredients were the same.

We used soybean protein isolate (SPI), palm oil, and konjac glucomannan (KGM), a highly viscous hydrophilic colloidal polysaccharides with strong water absorption capability, to create SEGs and DEGs. The KGM addition in the external aqueous phase was varied to achieve both gel types with the same content of each major component. The gel samples created from two different structural emulsions were analyzed using colorimetric, textural, rheological, oral tribological tests, microstructural observations, and sensory evaluations to investigate the differences in gel structure and properties. The results can provide guidance for adjusting and improving the emulsion gel structure and properties and applying DEGs as fat substitutes.

2. Materials and methods

2.1. Materials

The SPI (91.2% protein content and 5.1% ash, on a dry basis) was purchased from Shandong Yuwang Ecological Food Industry Co. Ltd., food-grade polyglycerol polyricinoleate (PGPR) (purity > 99%) was obtained from Beijing Jinlisi Technology Co. Ltd (Beijing, China). Food-grade sodium chloride (NaCl) (purity > 99%) was acquired from Henan Tianma Food Ingredients Co. Ltd. (Henan, China), while palm oil (46.85% saturated fatty acid content, 41.97% monounsaturated fatty acid, and 11.05% polyunsaturated fatty acid) was obtained from the Malaysian Palm Oil Board (MPOB). The KGM (from konjac powder with 90.1% KGM content and 0.84% ash, on a dry basis) was supplied by Hubei Yizhi Konjac Biotechnology Co. Ltd. (Hubei, China). The artificial saliva (ISO/TR10271, neutral), the Nile Blue and Nile Red fluorescent stains were purchased from Shanghai Yuanye Bio-Technology Co. Ltd (Shanghai, China). The Calcofluor White fluorescent staining kit (purity > 99%) was obtained from Separation Technology Co. Ltd (Beijing, China).

2.2. Preparation of the double emulsion

The water-in-oil-in-water ($W_1/O/W_2$) double emulsions were prepared following a two-step emulsification method described by Flaiz et al. (Flaiz, et al., 2016).The internal aqueous phase was comprised of 0.1 M NaCl solution. The oil phase was prepared by dissolving 8 wt% of PGPR in palm oil and stirring at 700 rpm for 10 min in a water bath at 65 °C. The external aqueous phase consisted of a 6% SPI solution, which was obtained by dissolving 6 wt% SPI powder in distilled water and stirring for 15 min at 25 °C until completely dissolved.

Firstly, the primary emulsion (W_1/O) was created through the subsequent procedures. The internal aqueous phase was gradually introduced to the oil phase (W_1:O = 4:6) while being strred using magnetic stirrer at 700 rpm for 10 min in a 65 °C water bath (LNB-HH-6A, HaoZhuang, Shanghai, China). The resulting mixture was homogenized at 15000 rpm for 10 min to obtain the W_1/O coarse emulsion by using a high-shear homogenizer (FJ200-SH, HUXI, Shanghai, China). Further refinement was achieved by passing the coarse emulsion through a high-pressure homogenizer (D-3L, PHD, USA) twice at 55/7 MPa and 25 °C, resulting in the formation of the primary emulsion (W_1/O).

Secondly, the primary emulsion (W_1/O) was added to the external aqueous phase (W_1/O:W_2 = 4:6). Then the mixture was subjected to a high-speed shear at 10000 rpm for 210 s by using a high-shear homogenizer to obtain the coarse double emulsion. Subsequently, the coarse double emulsion was subjected to two homogenization cycles at 15/3 MPa and 25 °C in the high-pressure homogenizer, leading to the formation of the double emulsion (W_1:O:W_2 = 1.6:2.4:6). To ascertain the successful formation of the double emulsion, the micromorphology of the samples was observed using an optical microscope by examining the W/O/W structures of the multiple compartments. The samples were refrigerated at 4 °C for 12 h for phase stabilization.

2.3. Preparation of the single emulsion

Single emulsion was formulated according to a method delineated by Huang et al. (Huang, et al., 2022). Briefly, SPI powder was dissolved in distilled water and stirred at 25 °C for 15 min by a magnetic stirrer (C-MAG HS7, IKA, Germany) until full dissolution was achieved to obtain an SPI solution with a concentration of 3.6%. Then, palm oil was added and stirred at 9000 rpm for 5 min, resulting in the formation of O/W single emulsion. It is worth noting that the ratios of all the major components were the same as in the double emulsion sample, contained 3.6% protein and 24% palm oil.

2.4. Preparation of the DEG and SEG

Basic emulsions were referred to as single or double emulsion without the addition of KGM (Konjac glucomannan). The KGM was systematically incorporated into the basic emulsions, resulting in the formation of emulsion gels. The process was carried out using a Thermomix food processor (Vorwerk, TM5, Wuppertal, Germany) set at a speed 2.5 for 4 min. Various levels of KGM were added: 3%, 5%, 7% and 9% for the single emulsion samples i.e., 3% SEG, 5% SEG, 7% SEG and 9% SEG and the double emulsions 3% DEG, 5% DEG, 7% DEG and 9% DEG, respectively. Following the KGM addition, the samples were placed in rectangular molds (11.6 cm × 8.2 cm × 3 cm) and degassed via evacuation at −0.09 MPa for 30 s (EXELWAY-300, LiDing, China). Subsequently, the samples were thermoregulated in water at 95 °C for 60 min, cooled to 25 °C, and refrigerated at 4 °C for 24 h to set for further analysis.

2.5. Scanning electron microscopy (SEM)

The emulsion gels were pre-treated separately according to a method described by Zhang et al. (Zhang, et al., 2021). The samples were cut into small pieces measuring 5 × 5 × 5 mm each and then carefully immersed in glutaraldehyde for 48 h to ensure proper fixation. Then, the samples underwent a thorough washing process, involving the four washes with 0.1 M PBS, followed by gradient dehydration and de-oiling using 30%, 50%, 70%, 90%, and 100% ethanol. Samples were pre-cooled and placed in a vacuum freeze dryer (Beta 1–8 LSC basic, Christ, Germany) until completely dry. The freeze-dried samples were sprayed and coated with thin layer of gold and then subjected to observation using an electron scanning microscope (S-4800, Hitachi, Japan) at 200x magnification. A representative field of view was selected for photography.

2.6. Chromaticity measurement

The chromaticity analysis of the samples was conducted using a colorimeter (CM-3610-A, Konica Minolta, Japan). The samples were cut into 3 × 3 × 1 cm cubes, and subjected to chromaticity measurement. To ensure accurate readings, the instrument was calibrated before the measurement using a standard white and black board. The CIE color values luminosity (L*), redness (a*), and yellowness (b*) were recorded for each sample. Each sample was subjected to six parallel determinations to minimize the potential for variability in the measurements. The ΔE was calculated using following formula.

$$\Delta E = \sqrt{(\Delta L^*)^2 + (\Delta a^*)^2 + (\Delta b^*)^2}$$

2.7. Confocal laser scanning microscopy (CLSM)

The microstructural observation of the emulsion gels was conducted using a CLSM (A1Rsi, Nikon, Japan) following a modified procedure based on the method outlined by Wei et al. (Wei, et al., 2021). Calcofluor White fluorescent, Nile Red, and Nile Blue stains were used for staining polysaccharides, oils and the proteins, respectively. The samples were cut into 3 × 4 × 1 mm slices using a scalpel and placed onto slides. 30 μL of 1% (w/w) Calcofluor White, 20 μL of 0.2% Nile Red, 20 μL of 0.5% Nile Blue was added to the sample successively and equilibrated in the dark for 30 min after each addition. The staining process involved successive additions of 30 μL of 1% (w/w) Calcofluor White, 20 μL of 0.2% Nile Red, and 20 μL of 0.5% Nile Blue to the samples. After each addition, the samples were allowed to equilibrate in darkness for 30 min. The stained samples were then covered with coverslips, fixed by wrapping the ends with sealing film, and observed via CLSM at 100x magnification. The excitation wavelengths of the three fluorescent stains were 355 nm, 488 nm, and 633 nm, respectively.

2.8. Texture profile analysis (TPA)

The texture profile was measured using a texture analyzer (CT3, Brookfield, Middleboro, USA) equipped with a TA10 probe (12.7 mm diameter). The samples were cut into 2 × 2 × 2 cm cubes and subject to axial compression. This compression process involved two cycles, each conducted at 1 mm/s speed with a trigger point load of 5 g to 40% of its original height, with 5 s interval between compression cycles. The change in load over time was recorded using the TexturePro CT software to obtain the hardness, springiness, cohesiveness, and chewiness values. Each sample was evaluated eight times.

2.9. Rheological analysis

The rheological behavior of the samples was investigated using an oscillatory rheometer (DHR-1, TA Instruments, New Castle, USA) in accordance with the approach outlined by Huang et al. (Huang, et al., 2022). The storage and loss modulus of the samples was assessed via amplitude, frequency, and temperature scanning. For analysis, a certain amount of emulsion gel sample was placed between the two plates of a 40 mm diameter plate jig. The upper plate was lowered slowly to a gap of 1 mm. Afterwards, the excess sample was removed using a scraper, while the plate edges were covered with dimethyl silicone oil to prevent moisture evaporation. The sample was equilibrated for 10 min before measurement at 37 °C. The amplitude scanning parameters included a strain γ ranged from 0.01% to 100% and an angular frequency of 10 rad/s. The amplitude scanning yielded a range of linear viscoelastic regions (LVR), from which a specific point (strain 1%) was selected for frequency and temperature scanning. The frequency scanning was conducted with in a frequency range of 1.0–10 Hz, while the temperature scanning was carried out within a temperature range of 40–100 °C, with a heating rate of 5 °C/min, and an angular frequency at 10 rad/s. The viscosity analysis included a shear rate range of 0.01 s^{-1} to 100 s^{-1}.

2.10. Oral tribology

Oral tribology of the samples was measured according to the method described by Huang et al. (Huang, et al., 2022) using a stress-controlled rheometer (DHR-1, TA Instruments, New Castle, USA) equipped with three-sphere geometry for simulating the upper jaw. 3M™ Transpore™ Surgical Tape was cut into squares and compacted tightly on the testing plat of the rheometer to simulate the rough surface of the tongue. After testing each sample, the tape was replaced with a new one to ensure consistent conditions. Subsequently, 3 g of the battered sample was mixed with 2 mL of artificial saliva to simulate the state of the food after chewing. The tests were performed at 37 °C, close to human body temperature. A test stress of 2 N was applied during the evaluation. The coefficient of friction was recorded at sliding speeds of 10^2 μm/s to 10^6 μm/s, and the measurements were repeated six times for each sample.

2.11. Sensory analysis

Sensory evaluation was carried out by following the method delineated by Jeong et al. (Jeong, et al., 2022). Each sample was cut into 3 × 2 × 1 cm rectangular pieces. These prepared samples were then assigned numbers and purposefully disordered to ensure unbiased assessments. The sensory evaluation panel was consisted of 15 food science students (eight females and seven males) with some experience in sensory analysis. The panelists sequentially tasted eight different samples, remaining unaware of the identity of each sample, and assigned scores to the samples based on various attributes, including overall appearance, chewiness, juiciness, oiliness, and acceptability. The scoring was conducted using a 9-point scale, with scores including “very poor and unacceptable” (1–3 points), “fair and acceptable” (4–6 points), and “excellent” (7–9 points). Following the evaluation of each sample, the sensory evaluators were instructed to rinse their mouths with water to avoid sensory fatigue and remove any lingering taste from the previous sample. All materials and equipment used for sample preparation were food-grade to ensure the safety of the imported samples. The sensory evaluation experiment was conducted with the informed consent of the sensory evaluation group members and was ethically approved by the Beijing Technology and Business University Scientific Research Ethics Committee (Ref. No. 21 of 2023).

2.12. Data analysis

The data were analyzed using IBM SPSS Statistics 27 for one-way analysis of variance (ANOVA) and Duncan’s multiple range test. The differences were considered significant at $p < 0.05$. The figures were plotted using the Origin 2022 software, and all measurements were performed at least three times.

3. Results and discussion

3.1. Observation of the appearance

As shown in Fig. 2, each sample exhibited a 3D cube shape with strong solid properties, suggesting their potential as cube fat mimetics. All the samples were a slightly yellowish milky white and faint yellow, which was consistent with the chromaticity results. At the same added KGM concentration, it was difficult to observe distinct differences between the DEG and SEG samples, while samples with different added KGM concentrations can be easily distinguished. The 3% KGM samples displayed a soft texture, rough surface, and directly observable pore-like network (the blue circles in Fig. 2). This could be because the polysaccharide network formed by the lower KGM concentration had difficulty supporting solid cube emulsion gel formation with large internetwork holes, making it challenging to shape the samples. As the added KGM concentration increased, the emulsion gel gradually exhibited smoother, finer surfaces, with a consequent reduction in hole structure and a firmer texture. The structural differences in the basic emulsions slightly affected the emulsion gel appearance at the same added KGM concentrations, while variations in the polysaccharide content significantly impacted the gel shape, with higher KGM levels making a more substantial contribution to 3D cube emulsion gel formation.

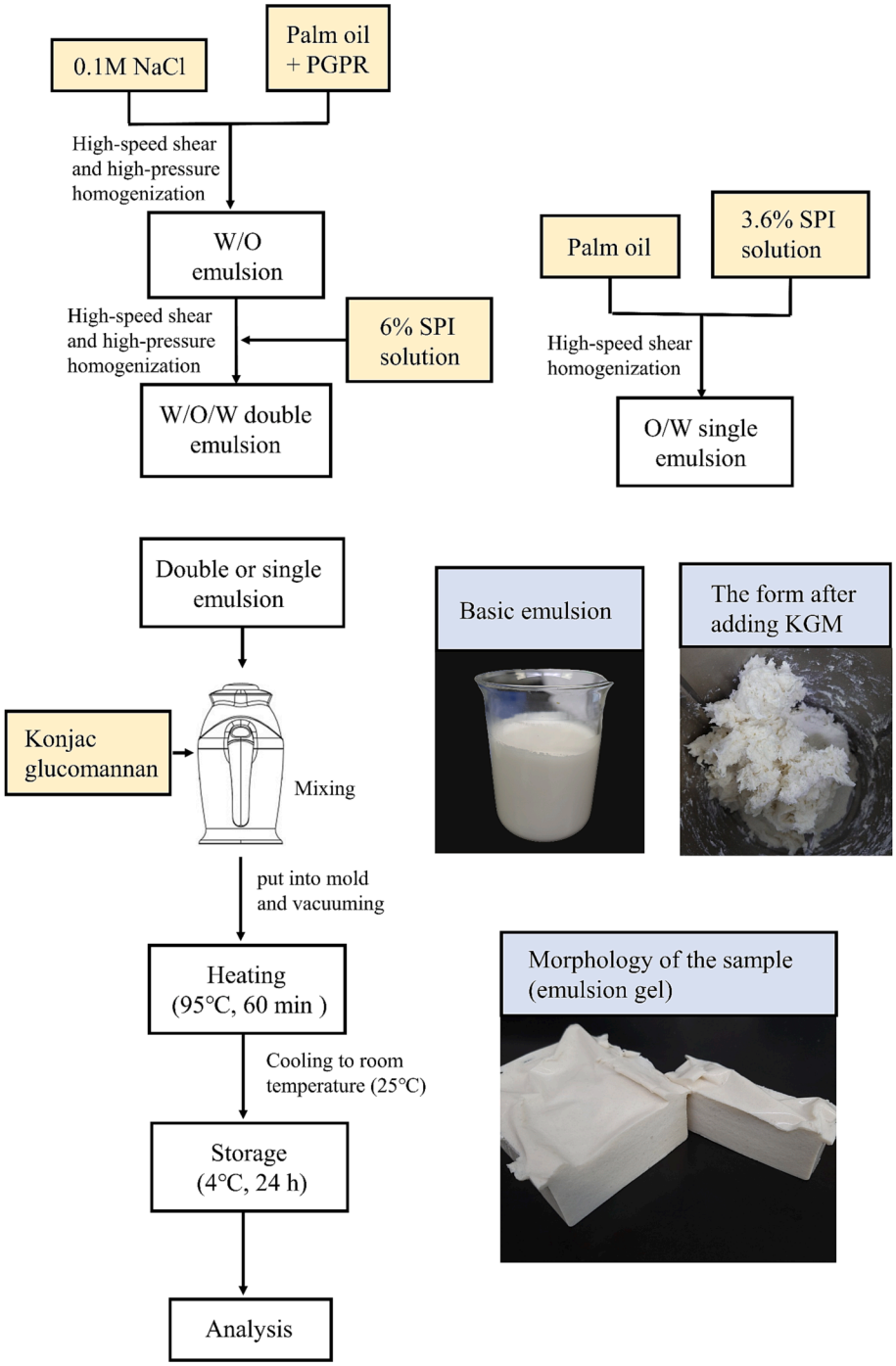

Fig. 1. The DEG and SEG sample preparation procedures.

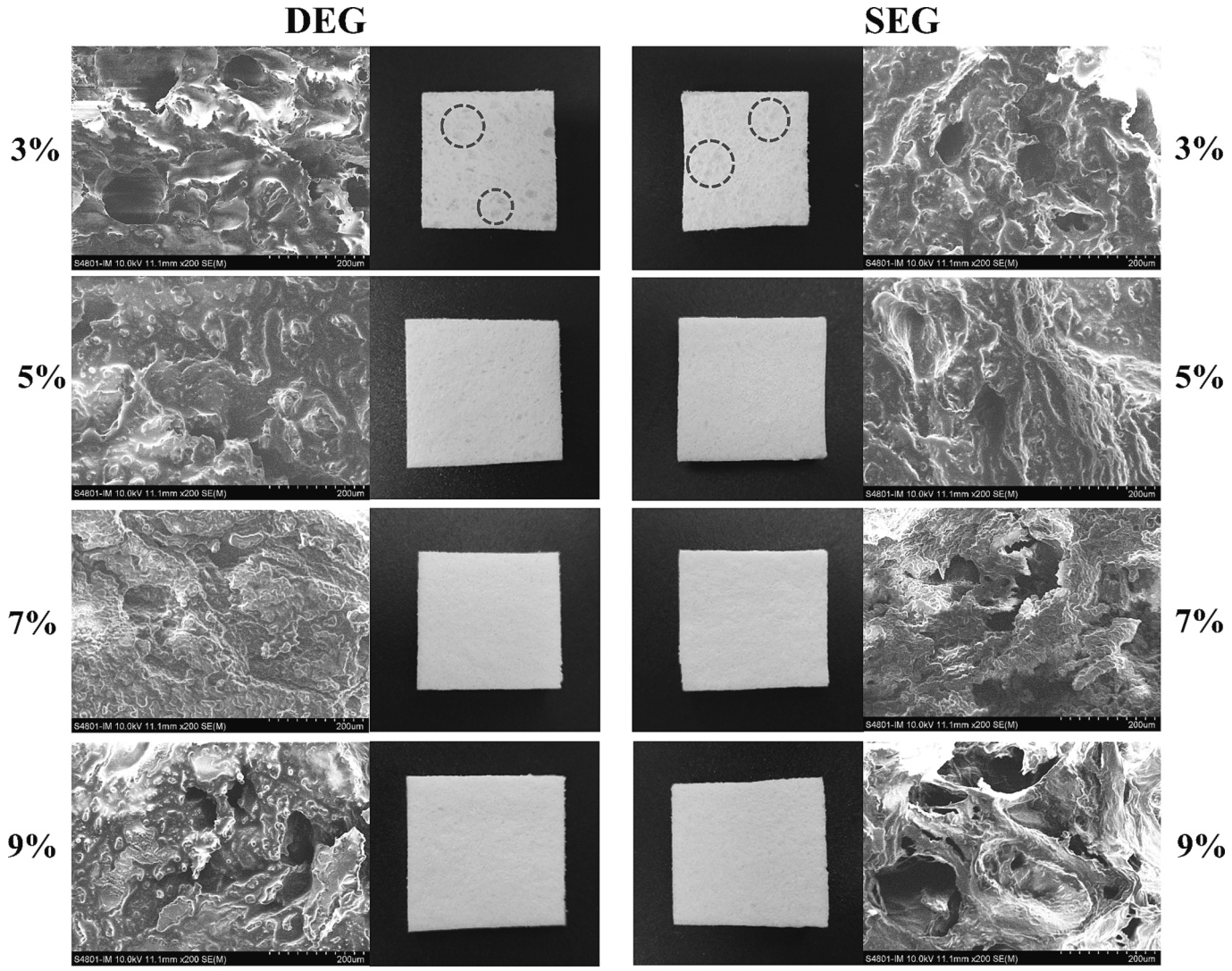

Fig. 2. The macroscopic morphological images and the SEM observation of SEG and DEG samples containing different added KGM concentrations. 3%, 5%, 7%, and 9% represent the KGM addition, while DEG and SEG represent the emulsion gels formed using double and single basic emulsions, respectively.

3.2. Chromaticity analysis

The color of fat in meat products may have an impact on consumers' purchasing desire. The parameters of the emulsification and gelation processes can induce substantial color differences in the emulsion gel, even when the types and concentrations of primary components (protein and oil) are consistent. Color changes in emulsion gels may be related to light reflection from small-diameter oil droplets, oxidation and denaturation of proteins, polysaccharides and oil properties (Jeong, Lee, Jo, & Choi, 2023). As shown in Table. 1, the L* value of the all the samples distributed in 88.93–92.73, which confirmed their bright milky white appearance. The b* value was in the range of 6.96–8.80 and a* values were close to zero, which might be due to the faint yellow KGM and palm oil used as raw materials. The L* value showed no significant difference ($p > 0.05$) between DEG and SEG with same added KGM concentration, except 9% DEG and 9% SEG. The increasing of KGM concentration caused a significantly decrease on L* value ($p < 0.05$), while did not significantly affect the a* and b* values ($p > 0.05$). This may be because

Table 1
The colorimetric and TPA results of the emulsion gel samples obtained using two emulsions containing different added KGM concentrations.

Sample	Chroma				TPA			
	L*	a*	b*	ΔE	Hardness (N)	Springiness (mm)	Cohesiveness	Chewiness (mJ)
3% DEG	92.57 ± 0.23^{a}	-0.31 ± 0.02^{a}	7.68 ± 0.09^{a}	—	1.57 ± 0.09^{a}	7.15 ± 0.34^{ac}	0.77 ± 0.02^{a}	8.67 ± 0.70^{ab}
3% SEG	92.73 ± 0.34^{a}	-0.33 ± 0.12^{ab}	8.05 ± 0.24^{b}	0.40	1.38 ± 0.11^{a}	6.74 ± 0.27^{a}	0.80 ± 0.01^{a}	7.45 ± 0.77^{a}
5% DEG	92.48 ± 0.19^{a}	-0.22 ± 0.03^{bc}	7.01 ± 0.18^{c}	0.67	4.04 ± 0.39^{b}	6.99 ± 0.28^{ac}	0.65 ± 0.06^{b}	18.23 ± 1.98^{c}
5% SEG	92.30 ± 0.57^{a}	-0.24 ± 0.02^{ac}	7.04 ± 0.20^{c}	0.69	4.54 ± 0.30^{b}	8.56 ± 2.94^{ac}	0.79 ± 0.01^{a}	27.97 ± 9.78^{bcdef}
7% DEG	91.34 ± 0.19^{b}	-0.08 ± 0.03^{d}	6.96 ± 0.16^{c}	1.44	5.93 ± 0.45^{c}	6.99 ± 0.30^{ac}	0.70 ± 0.05^{ab}	29.03 ± 1.61^{d}
7% SEG	90.99 ± 0.12^{b}	-0.10 ± 0.03^{d}	7.56 ± 0.07^{a}	1.60	7.68 ± 0.44^{d}	7.44 ± 0.12^{bc}	0.76 ± 0.07^{ab}	43.42 ± 4.56^{ef}
9% DEG	89.76 ± 0.15^{c}	-0.08 ± 0.02^{d}	8.24 ± 0.06^{b}	2.87	8.12 ± 0.61^{d}	7.02 ± 0.60^{ac}	0.70 ± 0.03^{b}	40.13 ± 8.35^{de}
9% SEG	88.93 ± 0.40^{d}	-0.07 ± 0.04^{d}	8.80 ± 0.18^{d}	3.82	9.27 ± 0.23^{e}	7.04 ± 0.16^{a}	0.72 ± 0.01^{b}	47.13 ± 1.31^{e}

Note: Different lowercase letters indicate significant differences ($p < 0.05$) in the groups.

higher KGM concentrations form a denser polysaccharide network that fills the holes in the protein network, forming the tighter gel surface that hinders light scattering and reduces the L* value.

ΔE represents a unit of color difference perceived by the human eye in a uniform color space. It is widely acknowledged that detecting color difference is challenging when $\Delta E < 1$, while trained or experienced individuals may perceive some variation when $1 < \Delta E < 2$. Consumers may notice color differences when $2 < \Delta E < 3.5$, while color differences are easily detectable when $3.5 < \Delta E < 5$ (Grobelna, Kalisz, & Kieliszek, 2019). The ΔE difference values between the DEG and SEG samples were less than 1 at the same added KGM concentration, indicating that the color difference between the emulsion gels obtained using the different basic emulsions was difficult to detect with the naked eye. The ΔE between the 3% and 9% SEG samples was the highest at a value of 3.82. This indicated that the influence of basic emulsion type on the color was slight. The color was mainly depended on the KGM concentration.

3.3. TPA

The texture profile of emulsion gels are important indicators of the gel structure. As shown in Table 1, the increasing concentration of KGM led to a significant increase in the hardness and chewiness of both the DEG and SEG ($p < 0.05$). However, it did not significantly affect the springiness and cohesiveness of the gel ($p > 0.05$). Several studies involving KGM-SPI composite gels (Huang et al., 2022; Ran & Yang, 2022) revealed that adding KGM increased the gel hardness and chewiness, mostly due to the removal of the acetyl group. This changed the KGM from a semi-curling to a self-curling state, leading to the formation of a 3D network with a rigid, compact structure (Ran, Lou, Zheng, Gu, & Yang, 2022). Higher KGM concentrations promoted the interaction with protein molecules, prolonged the time of protein denaturation, and facilitated the exposure of buried functional groups and protein aggregation, consequently encouraging the gel network formation, increasing composite gel strength, and enhancing the gel hardness and masticatory properties (Ran & Yang, 2022).

At higher KGM addition levels (7% and 9%), the hardness and chewiness of the DEG were substantially lower than the SEG ($p < 0.05$) at the same KGM concentration. No significant difference was found between the 7% SEG and 9% DEG ($p > 0.05$), despite the higher added KGM concentration in DEG. Indicated that SEG is more sensitive to KGM content changes than DEG. This could be because the basic double emulsion partially encapsulated water droplets as the inner water phase in the oil droplets, consequently exposing more water in the single emulsion than in the double emulsion with the same water content. KGM displays excellent thickening and water retention properties and is sensitive to the presence of water. The structural features of single emulsions enable the addition of KGM, which is highly viscous, to emulsions for increased water phase interaction, rapid water absorption, and agglomeration to create a viscous gel-like state that immobilizes oil droplets. The higher KGM concentrations in the 7% and 9% samples promoted water absorption to produce harder, chewier emulsion gels that differed significantly from DEG. This also suggests that the texture properties of emulsion gels can be adjusted by altering the structure of the basic emulsion.

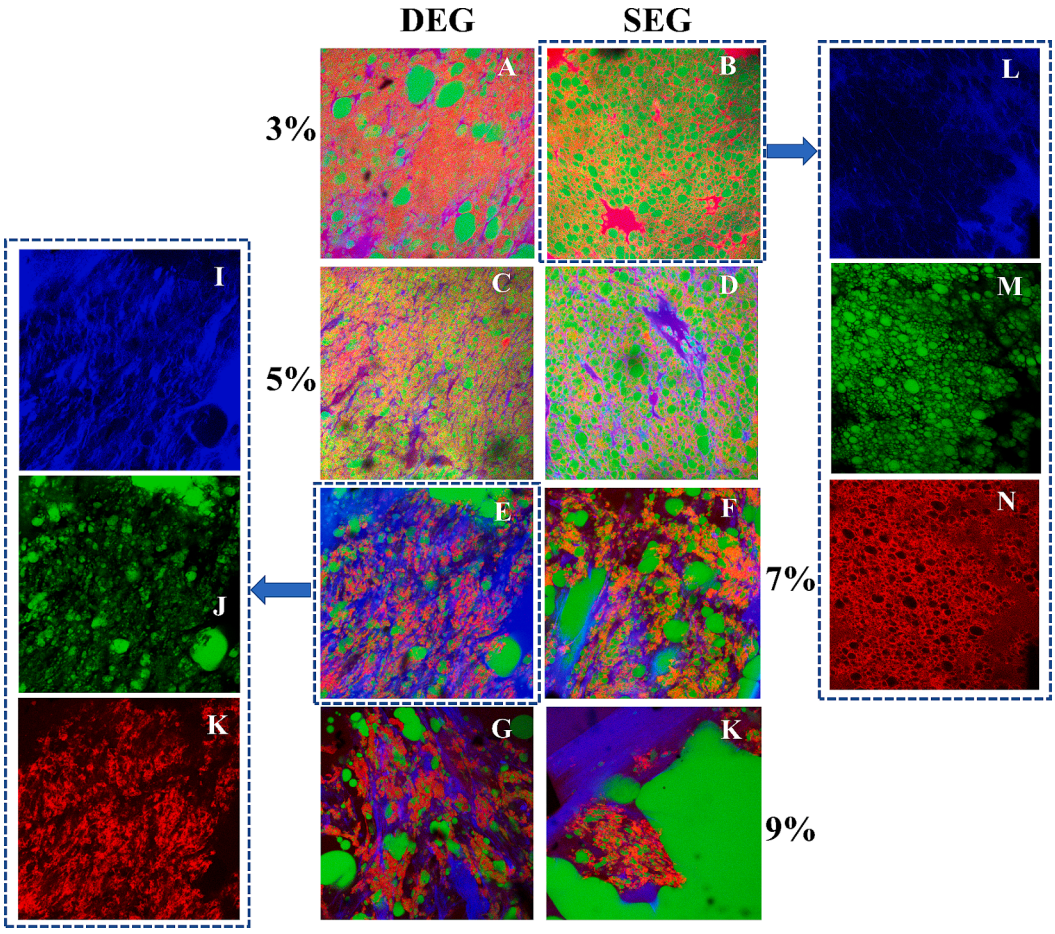

Fig. 3. The CLSM images of the emulsion gel samples obtained using two emulsions containing different KGM concentrations. A, B, C, D: the DEG samples at 3%, 5%, 7%, and 9% KGM concentrations. E, F, G, H: SEG samples at 3%, 5%, 7%, and 9% KGM concentrations. I, J, K, L, M, N: The single-channel images of the polysaccharides, lipids, and proteins for 7% DEG and 3% SEG, respectively. The blue fluorescence denotes polysaccharides, the green fluorescence represents lipids, and the red fluorescence signifies proteins. (For interpretation of the references to color in this figure legend, the reader is referred to the web version of this article.)

3.4. CLSM

The morphology and positional distribution of proteins, polysaccharides and oils in emulsion gels were observed using CLSM. Each sample (Fig. 3) displayed a distinct protein and polysaccharide network, with green fluorescent palm oil droplets embedded in the gel network, which was consistent with traditional emulsion-filled gel structures with protein-polysaccharide matrices (Ren, et al., 2022). The gradual increase in blue fluorescence indicates that higher added KGM concentrations promote denser polysaccharide network structures.

At 3% KGM, the oil droplet diameters in SEG were smaller and more uniformly dispersed than in DEG. This could be due to the larger oil droplets in the double emulsion resulting from the encapsulation of the internal water phase. Notably, not every oil droplet in the double emulsion successfully encapsulated a water droplet. The subsequent processing may have led to spillage of some internal water phase out of the oil phase into the external water phase, leading to a less uniform oil droplet distribution in DEG compared to SEG. The structural differences between the two emulsion gels were more evident in the samples containing high KGM concentrations. Oil droplet aggregation, larger droplets, and uneven distribution were evident in the 7% sample, while the 3% KGM sample showed the opposite trend. In the 9% SEG sample, the polysaccharide network formed by excess KGM was linked in sheets and no longer exhibited a fibrous network structure. The protein network was clearly agglomerated due to excess polysaccharide extrusion, with no apparent network structure. Severe oil droplet aggregation was evident, with no individual droplet dispersion in the gel network. The elastic modulus of the filled particles (oil droplets) is inversely proportional to the diameter of the droplets (Zhang et al., 2021). Excessively large oil droplets reduce the gel network strength, which may explain the significant hardness increase in the 9% SEG without a substantial rise in the storage modulus (G'). However, the same phenomenon was not observed in the 9% DEG. Compared to the 7% DEG, the protein and polysaccharide structures in the 9% DEG showed no significant changes. Although some oil droplet aggregation occurred, the overall structure was similar to the 7% SEG, which was also consistent with the hardness trend. This indicated that high KGM levels more significantly affected SEG, while DEG maintained a more stable oil droplet state and protein-polysaccharide network structure.

Fig. 3 I-N illustrate the variations in gel network between emulsion gels with low and high KGM levels. The polysaccharide network fluorescence intensity was weak at low KGM concentrations, revealing a distinctly homogeneous and porous protein network morphology. However, at high KGM concentrations, a shift in dominance occurred from protein to polysaccharide networks, with the aggregation of the protein network becoming pronounced. The oil droplet distribution gradually moved from the protein network to the polysaccharide network, which might be related to the differences between the DEG and SEG samples.

3.5. SEM

The 3D gel network structures of the DEG and SEG samples containing different amount of KGM were observed via SEM (Fig. 1). Overall, al the samples showed homogeneous surfaces. As added KGM concentrations increased, different structures exhibited in the gels. The 3% KGM sample surfaces displayed rounded edges with raised and depressed sections and fewer holes. The surfaces of the 5% KGM samples became flatter with fewer holes, probably due to the higher KGM content filling the protein network holes, as well as KGM and SPI interaction via hydrogen bond cross-linking, resulting in a denser composite gel network structure (Zhang, et al., 2022). Of all the samples, 7% DEG exhibited the flattest, densest gel surfaces with grooves, filled holes, and no apparent unnetworked particles, differing from the 7% SEG which displayed deeper grooves and holes. Significant structural gel network differences were evident at a 9% KGM concentration. The 9% DEG sample showed little change in the sizes and depths of the holes, while the particulate matter increased, possibly due to the failure of the KGM particles to form a network. This confirms the conclusion drawn from the textural and chromaticity results that excessive added KGM concentrations cause the lower external aqueous phase ratio of the double emulsion to restrict KGM network formation, preventing adequate water binding to produce a gel structure. Contrarily, distinctly deeper, larger holes were observed in the 9% SEG, with an overall netted structure. The CLSM results indicated that the low-concentration KGM samples primarily exhibited protein network gel structures, which gradually changed to polysaccharide networks as the KGM levels increased. This may also explain the significant differences between the morphological structures of the high and low KGM concentration samples. Since KGM displayed a high water binding capacity, the samples with this dominant network showed a distinct holey structure after vacuum freeze-drying, which was also similar to the microscopic morphology of KGM gels in other studies (Wang, et al., 2020). It has been suggested that structures with small holes display better absorption and water retention capacity than those with large holes (Tong, et al., 2018). The 9% SEG structure displayed the largest holes, which was consistent with the CLSM observation results. The excessive polysaccharide caused the blue fluorescing sections to be linked into sheets. The network with large holes prevented oil droplet retention, resulting in more severe oil droplet aggregation.

3.6. Rheological analysis

3.6.1. Amplitude scanning

The storage modulus (G') represents the energy stored due to elastic deformation, while the loss modulus (G'') denotes the energy lost due to viscous deformation. Amplitude scanning determines the extent of the LVR of a sample, where the G' and G'' are independent of the amplitude strain variation. As shown in Fig. 4A, all samples within the LVR exhibited the characteristics of gel-like materials as G' significantly exceeded G'' ($G'>G''$). The samples displayed a significant increase in G' and G'' at higher KGM concentrations, which was consistent with the findings of Ran et al. (Ran & Yang, 2022). This could be attributed to the significantly higher KGM content, which increased the structural strength of the SPI-KGM composite gels and the inter-chain interactions between KGM molecules, producing a more flexible, denser gel network. As the strain increased further, the G' decreased while the G'' increased. The two curves intersected, indicating that high strain caused irreversible damage to the emulsion gel network structure. Sample deformation is reversible in the LVR, while the maximum strain in the LVR is known as the critical strain (γ_L). A lower γ_L was observed in DEG than in SEG during amplitude scanning.

Increasing the added KGM concentration from 3% to 9% produced a four-fold higher G' in the DEG, which rose from 5.5 kPa to 21.5 kPa. For the SEG, the G' of the sample with 9% KGM was eight-fold higher than the 3% KGM, increasing from 3.5 kPa to 29.2 kPa. Furthermore, the G' and G'' of the DEG were higher than the SEG samples at a 3% KGM addition. The modulus curves of the two emulsion gels at 5% KGM almost overlapped, while both moduli were higher in the 7% and 9% KGM SEG samples than in the corresponding DEG samples. Higher KGM levels caused more obvious differences, which was consistent with the textural analysis results. The CLSM results showed that at low KGM concentrations, the emulsion gel network structures mainly consisted of protein networks, while heating caused protein denaturation and unfolding, exposing the hydrophobic residues inside and exhibiting highly negative electrostatic repulsion (O'Flynn, Hogan, Daly, O'Mahony, & McCarthy, 2021). During heat-induced protein gelation, hydrophobic group recombination leads to further protein molecule aggregation. This gelation process occurs in the exposed outer aqueous phase of the emulsion, with a smaller proportion of the aqueous phase exposed in the double emulsion, an environment that may promote protein aggregation, allowing stronger gel network formation and

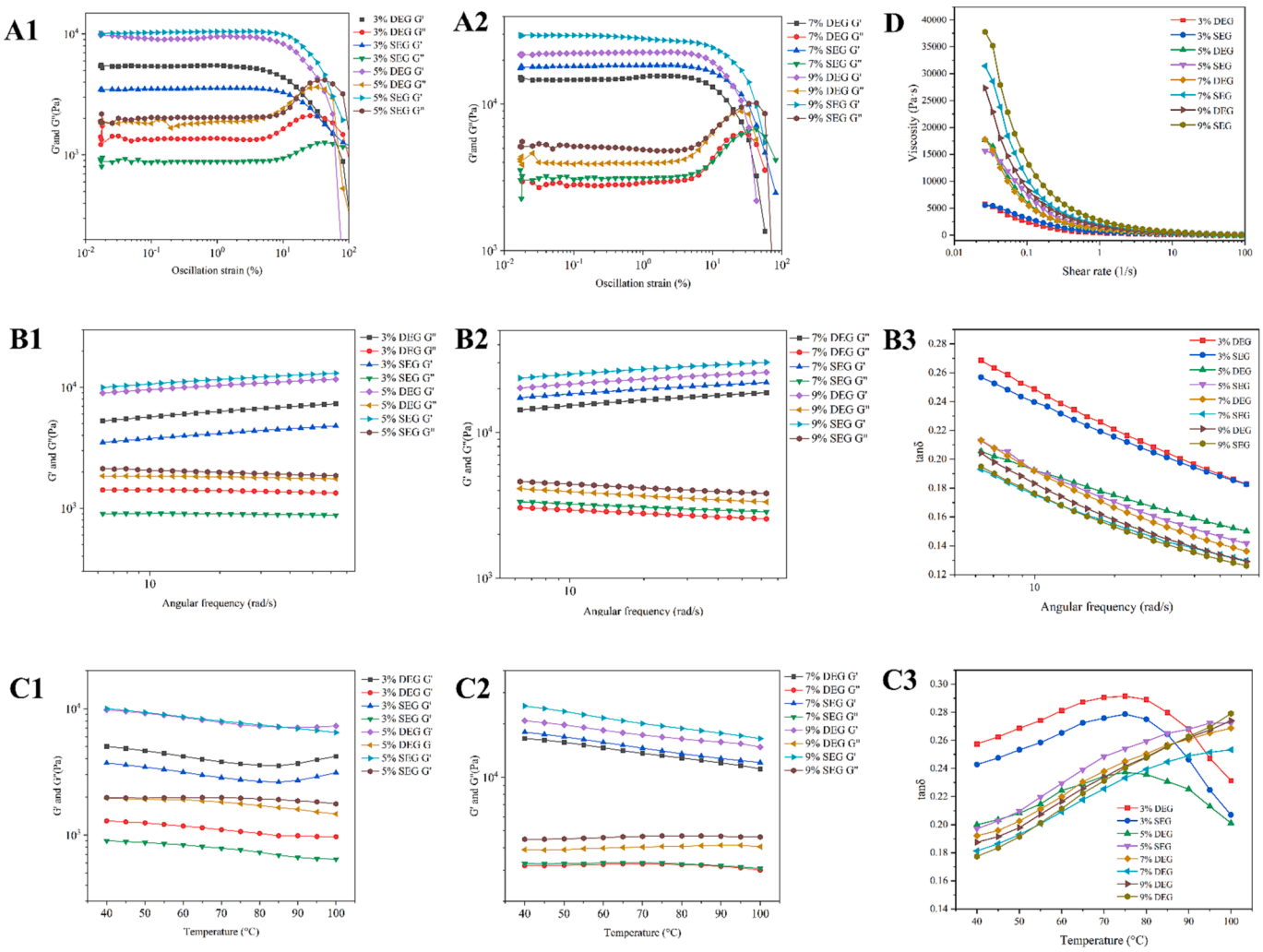

Fig. 4. The rheological test results for the emulsion gel samples obtained using two emulsions containing different added KGM concentrations. A1-A2: Amplitude scanning. B1-B2: Frequency scanning. B3: The damping factor (tan δ) obtained via frequency scanning. C1-C2: Temperature scanning. C3: The tan δ obtained via temperature scanning. D: Viscosity.

consequently exhibiting a higher energy *G'*. Contrarily, in samples containing high KGM concentrations, the polysaccharide network gradually replaced the proteins as the dominant gel network. KGM molecules exhibit excellent water absorption ability and high hydrophilicity due to the significant number of hydroxyl groups, allowing complete water absorption and swelling to form SEG gel networks displaying a higher proportion of external water phases. Furthermore, an increase in viscosity was observed, as well as a higher *G'*.

3.6.2. *Frequency scanning*

Fig. 4B shows the variation curves of the *G'* and *G"* as a frequency function for the samples, all of which exhibit solid properties (*G'* >*G"*). The trends exhibited by the DEG and SEG samples containing the same added KGM concentrations were also consistent with the amplitude scanning results. Although the *G'* of the samples increased slightly at a higher frequency, the overall trend was stable with little frequency dependence. The tan δ variation was determined using the frequency scanning results. Tan δ is usually defined as *G'* to *G''* ratio and reflects the nature of the gel network. A smaller tan δ signifies a stronger elastic gel network structure. To obtain a strong gel, the *G'* must be at least 10-fold higher than the *G"*, which means tan $\delta < 0.1$. The gel samples in this study all exhibited tan δ values between 0.1 and 0.3, while the *G'* and *G"* frequency dependence was insignificant, which was consistent with weak gels (Fan, Cheng, Zhang, Zhang, & Han, 2022). At higher added KGM concentrations, the tan δ values of the samples gradually decreased and showed stronger gel properties. KGM is often used as a plasticizer due to its substantial water absorption capability. A higher KGM content and gelling behavior promote hydrogen bonding and hydrophobic interaction between KGM and SPI molecules, resulting in a denser, stronger gel structure. Moreover, the stronger gel properties make the samples less vulnerable to irreversible deformation under increased strain, which could also explain the higher γ_L in the SEG samples than in the DEG samples during amplitude scanning.

3.6.3. *Temperature scanning*

All samples exhibited a slight decline in *G'* at higher temperatures, while the curve remained stable and solid characteristics (*G'* > *G''*), indicative of thermal irreversibility without high-temperature melting. This behavior may be attributed to heat-induced SPI gelation. Even at high temperatures, the KGM and SPI composite gel network maintained stable solid gel properties. For the samples with 3% and 5% KGM, the *G'* of the emulsion gel decreased slightly between 40 °C and 85 °C, followed by a slight increase. This may be because most of the gel structure formed by the SPI network occurs at low KGM concentrations, increasing the temperature for SPI glass transition. It may also be attributed to the higher probability of intermolecular collisions due to higher temperatures, promoting KGM and SPI molecule cross-linking to form a composite gel network, which increases the *G'*. Studies have

shown (Wu, Hua, Chen, Kong, & Zhang, 2017) that the proportion of non-network proteins in SPI gels decreases at higher temperatures while decreasing substantially above 85 °C, with the lowest value at 100 °C. This was consistent with the temperature scanning results of the 3% and 5% KGM samples. However, this trend was not observed in the 7% and 9% KGM samples, probably because the gel structure was dominated by a polysaccharide network due to high KGM concentrations, completely filling the protein gel network and increasing the gel strength. Therefore, the effect of heating on the protein structure was masked, resulting in overall *G'* stability.

3.6.4. Viscosity

Fig. 4D illustrated the apparent viscosity of the samples as influenced by shear rate. All the samples showed a shear-thinning behavior, apparent viscosity decreased with increased shear rate. The continuous phase viscosity of the emulsion and the polymer adsorption at the oil–water interface were vital for stabilizing the internal oil droplets (Kuang, et al., 2023). This decrease in viscosity may be due to the disruption of the gel structure or oil droplet morphology at high shear rates. A stronger gel increased the apparent viscosity of samples, which was related to the higher weight-average molar mass of the KGM (Qiao, Shi, Luo, Jiang, & Zhang, 2022). KGM is often used as a thickening agent in food due to its strong water absorption ability and high viscosity. Therefore, the samples containing higher KGM concentrations were more viscous and displayed more significant water absorption for gel formation. The viscosity variation between the DEG and SEG samples at the same KGM concentration was consistent with the amplitude scanning results.

3.7. Oral tribology

Oral tribology was used to understand the lubrication mechanisms of emulsion gels in simulated oral environments. As shown in Fig. 5 (A), the friction curves of the samples were approximately the same, with distinct double-peaked distribution. Although they differed from the classic Stribeck curve, they were consistent with the friction curves in some related hydrophilic gel studies. This double-peaked friction curve can be divided into three zones (Pondicherry, Rummel, & Laeuger, 2019): the low sliding speed zone, where the friction coefficient increases with the sliding speed (slope of the curve > 0), the medium sliding speed zone, where the friction coefficient decreases and then increases in samples with high fat content, and the high sliding speed zone where the friction coefficient decreases with the sliding speed (slope of the curve < 0).

With increased KGM concentrations, the friction curves of the samples noticeably shifted upwards and the friction coefficient was increased. This phenomenon can be attributed to the substantial size of the KGM particles, coupled with their strong water-binding capabilities. Higher concentrations also increased the sample's viscosity, thereby diminishing the sensation of lubrication within the oral environment. Furthermore, a more significant KGM quantity was interlinked with the protein to reinforce the gel networks, increasing the textural hardness and friction coefficient. Compared to the structural differences in the basic emulsion, the added KGM concentration variation more substantially affected the friction coefficient of the emulsion gel samples. A higher added KGM concentration resulted in a rougher mouthfeel, which was also consistent with the lower juiciness and oiliness scores of the samples during the sensory evaluation analysis.

The curves of the samples with the same KGM level were compared to investigate the lubricity property differences between the emulsion gels obtained using different basic emulsion structures. A comparison between the 3% KGM samples indicated that their friction coefficients were almost identical in the low sliding speed zone, while the SEG samples showed a lower friction coefficient in the high sliding speed zone. The 5% DEG and 5% SEG samples exhibited similar lubrication properties, with almost overlapping friction curves. However, at high KGM concentrations, the friction curves of the DEG samples were lower than SEG, exhibiting smaller friction coefficients and better lubrication properties. No significant differences were evident between the SEG and DEG friction curves in the low sliding speed zone, while both showed higher friction coefficients due to the slippery problem at the beginning of the test (Zhu, Bhandari, & Prakash, 2018). The thickening of the lubricating film on the surface via partial separation friction reduced the friction coefficient in the medium sliding speed zone (Zhao, Bhandari, Gaiani, & Prakash, 2023), while the free lipids released from the gel matrices formed a thick oily film, which acted as a lubricant (Zhang et al., 2022). The difference between DEG and SEG samples was differentiated by the oil droplet encapsulation of the inner aqueous phase of DEG. The increased sliding speed may also prompt the oil droplets in the DEG matrix to release internal water droplets into the external aqueous phase during the release process to act as a lubricant in conjunction with the free lipids. Therefore, DEG exhibited a lower friction coefficient than the SEG samples, which was consistent with the conclusions presented in a study by Oppermann et al. (Oppermann, Verkaaik, Stieger, & Scholten, 2017). Moreover, they suggested that the PGPR emulsifier in the double emulsion might adsorb to the

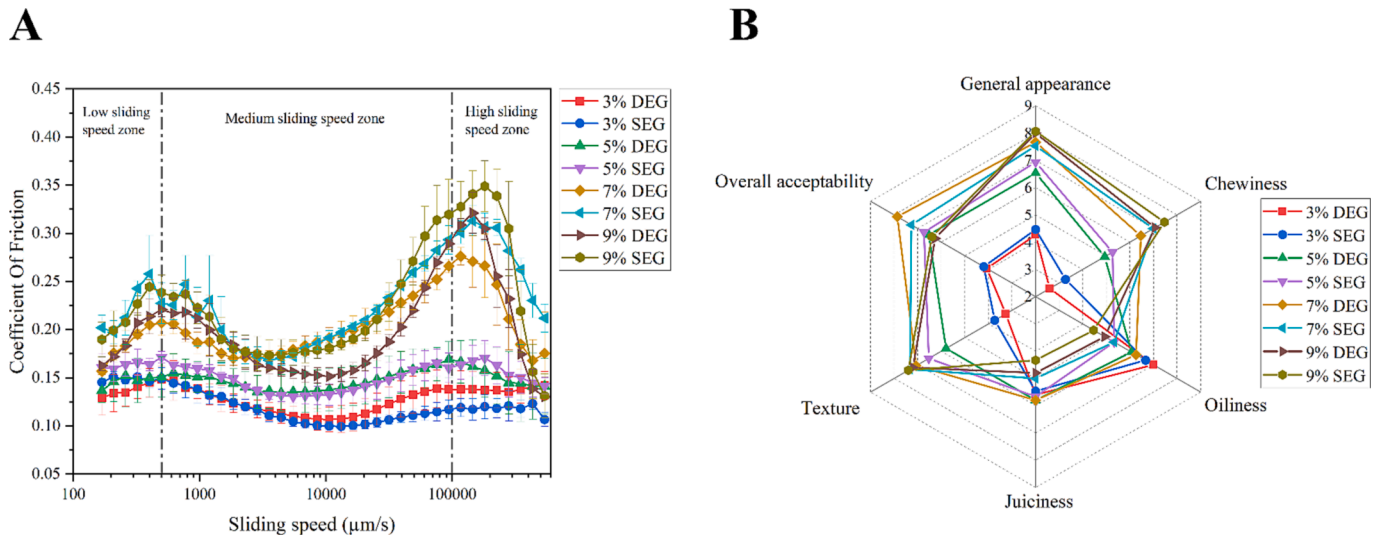

Fig. 5. The friction curves (A) and the sensory evaluation scores (B) of the emulsion gel samples obtained using two emulsions containing different KGM concentrations.

hydrophobic friction surface to reduce the friction at low sliding speeds. Although more protein and polysaccharide matrices were entrained into the contact zone under the influence of the sliding speed, increasing the friction, the unique DEG structure resulted in lower friction curves than the SEG samples. Finally, in the high sliding speed zone, further gel matrix breakdown led to the aggregation of released oil and water, which had a lubricating effect and reduced the friction coefficient, corresponding to the results of several previous studies (Li, Chen, Hao, & Xu, 2023; Mu, Ren, Shen, Zhou, & Luo, 2022). Therefore, due to the same content of each major component in the double emulsion and its unique multi-compartment structure, the DEG exhibited better oral lubrication properties and a lower friction coefficient than SEG.

3.8. Sensory evaluation

As shown in Fig. 5 (B), the 3% KGM samples displayed exceedingly low acceptable appearance and hardness levels. Although these samples exhibited good juiciness and oiliness, they lacked chewiness and were unsuitable as cube fat mimetics to provide mouthfeel. The appearance, chewiness, and texture scores of the samples increased significantly at higher added KGM concentrations ($p < 0.05$), while the oiliness and juiciness scores decreased considerably. Therefore, higher KGM levels resulted in a firm, dense emulsion gels, while the substantial hardness of the samples was preferred by the sensory evaluators. The strong water absorption and water retention capacity of KGM caused the samples to release less water when chewed (Ruiz-Capillas, Triki, Herrero, Rodriguez-Salas, & Jimenez-Colmenero, 2012), reducing the juiciness score. In the sensory evaluation, oiliness usually refers to the intensity of the fatty or oily feeling of the samples in the mouth and whether they provide a smooth feeling and form a coating on the palate (Fuhrmann, Sala, Stieger, & Scholten, 2020). As the oil droplets in the emulsion and the water droplets in the internal water phase are encapsulated by the dense polysaccharide network structure and filled in, the oiliness scores of the samples reduce accordingly. Several previous studies (Huang, et al., 2022a; Huang, et al., 2022b) showed that higher KGM content or dense polysaccharide network formation decreased the juiciness scores of gel samples while incorporating fat mimetics into meat products as a significant fat replacement decreased the juiciness.

At the same added KGM concentration, the SEG samples yielded higher chewiness and texture scores, while the DEG samples scored higher in terms of juiciness and oiliness, which was consistent with the texture and oral tribology results. Consequently, emulsion gel samples obtained using two differently structured basic emulsions displayed their own unique characteristics. With the same content of major components, DEG exhibited more oil–water feeling than SEG. But the hardness and chewiness of DEG were weaker. It has been suggested that uneven oil droplet distribution may impact the sensory properties of emulsion-filled gels(Fuhrmann, Sala, Stieger, & Scholten, 2020), especially the hardness and oiliness. The CLSM results indicated more uniform oil droplet distribution in the SEG samples than in the DEG samples. This may be caused by a combination of uneven oil droplet distribution, a lower oral friction coefficient, and the specific release characteristics of oil droplets and internal water phases. Therefore, the sensory attributes of emulsion gels can be adjusted by changing the structure of the basic emulsion, depending on their needs. The 7% DEG scored significantly higher than the other samples in the overall acceptability scores. This sample displayed better oiliness, juiciness, hardness, chewiness, and gel strength.

4. Conclusion

This study prepared SPI-KGM composite-based emulsion gels using double emulsion (W/O/W) and single emulsion (O/W) with variation of KGM addition. And the differences on their gel structures were investigated. KGM addition had a strong impact on the double and single emulsion gels. Samples with high KGM levels yielded higher hardness, chewiness, gel strength, oral friction coefficients. Higher appearance and texture scores, lower oily and juiciness scores were received in the sensory evaluation. The gel properties of the samples with different emulsion structure were almost identical at low KGM concentrations. The properties of SEG were more sensitive to KGM concentration at high KGM levels. At the same major component content, SEG exhibited better chewiness and a firmer texture than DEG, which displayed a lower oral friction coefficient and higher juiciness and oiliness, making it more suitable for using as a solid cube fat mimetic. These properties were particularly evident in the 7% DEG sample, which was a 22.85% lower in hardness, 33.14% lower in chewiness, and 1.14 scores higher in oiliness score compared to the 7% SEG. No significant differences were founded between the two emulsions in terms of appearance and chromaticity ($p > 0.05$). In addition, the unique multiple-compartment structure of the double emulsion offers the possibility of encapsulating pigments, flavoring substances, or functional ingredients and provides a basis for developing new fat substitutes. Further research should regarding gelled double emulsions as cube fat mimetics and conducted to develop fat mimetics with oiliness and sensory properties closer to real meat fats.

Author statement

This is an original paper that has not been published elsewhere and is not currently being considered by another journal in whole or in part. All authors have seen a draft copy of the revised manuscript and agreed to its publication. Yuqing Ren and Lai Wei performed the experiments and wrote the paper; He Li designed the experiments, reviewed and edited the manuscript; Jun Hao Yoong and Zhiyue Miao conceived the experiment and analyzed the data; Jinnuo Cao and Xinqi Liu provided scientific guidance. All authors read and approved the manuscript.

Declaration of Competing Interest

The authors declare that they have no known competing financial interests or personal relationships that could have appeared to influence the work reported in this paper.

Data availability

Data will be made available on request.

Acknowledgments

The research was supported by the National Key Research and Development Program of China (2021YFC2101405); the fund of Cultivation Project of Double First-Class Disciplines of Food Science and Engineering, Beijing Technology & Business University (No. BTBUYXTD202203).

Appendix A. Supplementary material

Supplementary data to this article can be found online at https://doi.org/10.1016/j.foodchem.2023.137450.

References

Chen, J. X., Zhao, J. H., Li, X., Liu, Q., & Kong, B. H. (2021). Composite gel fabricated with konjac glucomannan and carrageenan could be used as a cube fat substitute to partially replace pork fat in harbin dry sausages. *Foods, 10*(7). https://doi.org/10.3390/foods10071460

Chen, M. M., Li, W. T., Wang, W. B., Cao, Y., Lan, Y. Q., Huang, Q. R., & Xiao, J. (2022). Effects of gelation on the stability, tribological properties and time-delayed release profile of double emulsions. *Food Hydrocolloids, 131*. https://doi.org/10.1016/j.foodhyd.2022.107753

Dickinson, E., Radford, S. J., & Golding, M. (2003). Stability and rheology of emulsions containing sodium caseinate: Combined effects of ionic calcium and non-ionic surfactant. *Food Hydrocolloids, 17*(2), 211–220. https://doi.org/10.1016/s0268-005x(02)00055-3

Eisinaite, V., Juraite, D., Schroen, K., & Leskauskaite, D. (2017). Food-grade double emulsions as effective fat replacers in meat systems. *Journal of Food Engineering, 213*, 54–59. https://doi.org/10.1016/j.jfoodeng.2017.05.022

Fan, Z. P., Cheng, P., Zhang, P., Zhang, G. M., & Han, J. (2022). Rheological insight of polysaccharide/protein based hydrogels in recent food and biomedical fields: A review. *International Journal of Biological Macromolecules, 222*, 1642–1664. https://doi.org/10.1016/j.ijbiomac.2022.10.082

Flaiz, L., Freire, M., Cofrades, S., Mateos, R., Weiss, J., Jimenez-Colmenero, F., & Bou, R. (2016). Comparison of simple, double and gelled double emulsions as hydroxytyrosol and n-3 fatty acid delivery systems. *Food Chemistry, 213*, 49–57. https://doi.org/10.1016/j.foodchem.2016.06.005

Freire, M., Cofrades, S., Serrano-Casas, V., Pintado, T., Jimenez, M. J., & Jimenez-Colmenero, F. (2017). Gelled double emulsions as delivery systems for hydroxytyrosol and n-3 fatty acids in healthy pork patties. *Journal of Food Science and Technology-Mysore, 54*(12), 3959–3968. https://doi.org/10.1007/s13197-017-2860-9

Fuhrmann, P. L., Sala, G., Stieger, M., & Scholten, E. (2020). Effect of oil droplet inhomogeneity at different length scales on mechanical and sensory properties of emulsion-filled gels: Length scale matters. *Food Hydrocolloids, 101*. https://doi.org/10.1016/j.foodhyd.2019.105462

Grobelna, A., Kalisz, S., & Kieliszek, M. (2019). the effect of the addition of blue honeysuckle berry juice to apple juice on the selected quality characteristics, anthocyanin stability, and antioxidant properties. *Biomolecules, 9*(11). https://doi.org/10.3390/biom9110744

Heck, R. T., Saldana, E., Lorenzo, J. M., Correa, L. P., Fagundes, M. B., Cichoski, A. J., … Campagnol, P. C. B. (2019). Hydrogelled emulsion from chia and linseed oils: A promising strategy to produce low-fat burgers with a healthier lipid profile. *Meat Science, 156*, 174–182. https://doi.org/10.1016/j.meatsci.2019.05.034

Herrero, A. M., & Ruiz-Capillas, C. (2021). Novel lipid materials based on gelling procedures as fat analogues in the development of healthier meat products. *Current Opinion in Food Science, 39*, 1–6. https://doi.org/10.1016/j.cofs.2020.12.010

Huang, L., Ren, Y., Li, H., Zhang, Q., Wang, Y., Cao, J., & Liu, X. (2022). Create fat substitute from soybean protein isolate/Konjac glucomannan: the impact of the protein and polysaccharide concentrations formulations. *Frontiers in Nutrition, 9*, Article 843832. https://doi.org/10.3389/fnut.2022.843832

Huang, L., Zhao, D., Wang, Y., Li, H., Zhou, H. C., & Liu, X. Q. (2022). Transglutaminase treatment and pH shifting to manipulate physicochemical properties and formation mechanism of cubic fat substitutes. *Food Chemistry-X, 16*. https://doi.org/10.1016/j.fochx.2022.100508

Jeong, H., Kim, H., Lee, J. S., Jo, Y. J., Choi, M. J., & Ko, E. Y. (2022). Physico-Chemical properties and storage stability of an emulsion as a fat replacer in meat analogs during the freezing storage. *Foods, 11*(24). https://doi.org/10.3390/foods11243977

Jeong, H., Lee, J. S., Jo, Y. J., & Choi, M. J. (2023). Thermo-irreversible emulsion gels based on deacetylated konjac glucomannan and methylcellulose as animal fat analogs. *Food Hydrocolloids, 137*. https://doi.org/10.1016/j.foodhyd.2022.108407

Jimenez-Colmenero, F., Salcedo-Sandoval, L., Bou, R., Cofrades, S., Herrero, A. M., & Ruiz-Capillas, C. (2015). Novel applications of oil-structuring methods as a strategy to improve the fat content of meat products. *Trends in Food Science & Technology, 44*(2), 177–188. https://doi.org/10.1016/j.tifs.2015.04.011

Kuang, Y., Zhao, S., Liu, P., Liu, M., Wu, K., Liu, Y., … Jiang, F. (2023). Schiff base type casein-konjac glucomannan conjugates with improved stability and emulsifying properties via mild covalent cross-linking. *Food Hydrocolloids, 141*, Article 108733. https://doi.org/10.1016/j.foodhyd.2023.108733

Kumar, Y., & Kumar, V. (2020). Effects of double emulsion (W1/O/W2) containing encapsulated murraya koenigii berries extract on quality characteristics of reduced-fat meat batter with high oxidative stability - ScienceDirect. *Lwt-Food Science and Technology, 127*, Article 109365. https://doi.org/10.1016/j.lwt.2020.109365

Lang, Z., Yingying, H., Hussain Badar, I., Xiufang, X., Baohua, K., & Qian, C. (2021). Prospects of artificial meat: Opportunities and challenges around consumer acceptance. *Trends in Food Science & Technology, 116*, 434–444. https://doi.org/10.1016/j.tifs.2021.07.010

Li, X., Chen, W., Hao, J., & Xu, D. (2023). Construction of different properties single and double cross-linked binary emulsion filled gels based on rice bran oil body emulsion. *Colloids and Surfaces A: Physicochemical and Engineering Aspects, 665*, Article 131238. https://doi.org/10.1016/j.colsurfa.2023.131238

Mu, S., Ren, F. Z., Shen, Q. W., Zhou, H., & Luo, J. (2022). Creamy mouthfeel of emulsion-filled gels with different fat contents: Correlating tribo-rheology with sensory measurements. *Food Hydrocolloids, 131*. https://doi.org/10.1016/j.foodhyd.2022.107754

Nacak, B., Ozturk-Kerimoglu, B., Yildiz, D., Cagindi, O., & Serdaroglu, M. (2021). Peanut and linseed oil emulsion gels as potential fat replacer in emulsified sausages. *Meat Science, 176*, 9. https://doi.org/10.1016/j.meatsci.2021.108464

O'Flynn, T. D., Hogan, S. A., Daly, D. F. M., O'Mahony, J. A., & McCarthy, N. A. (2021). Rheological and solubility properties of soy protein isolate. *Molecules, 26*(10). https://doi.org/10.3390/molecules26103015

Oppermann, A. K. L., Verkaaik, L. C., Stieger, M., & Scholten, E. (2017). Influence of double (w(1)/o/w(2)) emulsion composition on lubrication properties. *Food & Function, 8*(2), 522–532. https://doi.org/10.1039/c6fo01523a

Pondicherry, K. S., Rummel, F., & Laeuger, J. (2019). Extended stribeck curves for food samples. *Biosurface and Biotribology, 4*(1), 34–37. https://doi.org/10.1049/bsbt.2018.0003

Qiao, D. L., Shi, W. J., Luo, M., Jiang, F. T., & Zhang, B. J. (2022). Polyvinyl alcohol inclusion can optimize the sol-gel, mechanical and hydrophobic features of agar/konjac glucomannan system. *Carbohydrate Polymers, 277*. https://doi.org/10.1016/j.carbpol.2021.118879

Ran, X. L., Lou, X. W., Zheng, H. Q., Gu, Q. Y., & Yang, H. S. (2022). Improving the texture and rheological qualities of a plant-based fishball analogue by using konjac glucomannan to enhance crosslinks with soy protein. *Innovative Food Science & Emerging Technologies, 75*, Article 102910. https://doi.org/10.1016/j.ifset.2021.102910

Ran, X. L., & Yang, H. S. (2022). Promoted strain-hardening and crystallinity of a soy protein-konjac glucomannan complex gel by konjac glucomannan. *Food Hydrocolloids, 133*. https://doi.org/10.1016/j.foodhyd.2022.107959

Ren, Y. Q., Huang, L., Zhang, Y. X., Li, H., Zhao, D., Cao, J. N., & Liu, X. Q. (2022). Application of emulsion gels as fat substitutes in meat products. *Foods, 11*(13). https://doi.org/10.3390/foods11131950

Ruiz-Capillas, C., Triki, M., Herrero, A. M., Rodriguez-Salas, L., & Jimenez-Colmenero, F. (2012). Konjac gel as pork backfat replacer in dry fermented sausages: Processing and quality characteristics. *Meat Science, 92*(2), 144–150. https://doi.org/10.1016/j.meatsci.2012.04.028

Tong, Q. Y., Chen, L., Wang, W. J., Zhang, Z. P., Yu, X. P., & Ren, F. (2018). Effects of konjac glucomannan and acetylated distarch phosphate on the gel properties of pork meat myofibrillar proteins. *Journal of Food Science and Technology-Mysore, 55*(8), 2899–2909. https://doi.org/10.1007/s13197-018-3208-9

Wang, Y. L., Han, L., Yan, J., Hu, K., Li, L. H., Zhang, H., & Ai, H. (2020). 3D bioprintability of konjac glucomannan hydrogel. *Materials Science-Medziagotyra, 26*(1), 109–113. https://doi.org/10.5755/j01.ms.26.1.20336

Wei, R. J., Zhao, S. J., Zhang, L., Feng, L. P., Zhao, C. Y., An, Q., … Zheng, J. K. (2021). Upper digestion fate of citrus pectin-stabilized emulsion: An interfacial behavior perspective. *Carbohydrate Polymers, 264*. https://doi.org/10.1016/j.carbpol.2021.118040

Wu, C., Hua, Y. F., Chen, Y. M., Kong, X. Z., & Zhang, C. M. (2017). Effect of temperature, ionic strength and 11S ratio on the rheological properties of heat-induced soy protein gels in relation to network proteins content and aggregates size. *Food Hydrocolloids, 66*, 389–395. https://doi.org/10.1016/j.foodhyd.2016.12.007

Zhang, Q., Yin, L. J., Chen, F. S., Zhang, P. L., Lv, D. Y., Zhu, T. W., & Duan, X. J. (2021). Effect of soybean oil content on textural, rheological, and microstructural properties of WBAXs-SPI emulsion-filled gels. *Journal of Texture Studies, 52*(2), 251–259. https://doi.org/10.1111/jtxs.12581

Zhang, Q. B., Huang, L., Li, H., Zhao, D., Cao, J. N., Song, Y., & Liu, X. Q. (2022). Mimic pork rinds from Plant-Based gel: the influence of sweet potato starch and konjac glucomannan. *Molecules, 27*(10). https://doi.org/10.3390/molecules27103103

Zhang, X., Chen, X., Gong, Y. H., Li, Z. Y., Guo, Y. F., Yu, D. A. Y., & Pan, M. Z. (2021). Emulsion gels stabilized by soybean protein isolate and pectin: Effects of high intensity ultrasound on the gel properties, stability and 13-carotene digestive characteristics. *Ultrasonics Sonochemistry, 79*. https://doi.org/10.1016/j.ultsonch.2021.105756

Zhang, Y. H., Wang, Y. C., Zhang, R. N., Yu, J. J., Gao, Y. X., & Mao, L. K. (2022). Tuning the rheological and tribological properties to simulate oral processing of novel high internal phase oleogel-in-water emulsions. *Food Hydrocolloids, 130*. https://doi.org/10.1016/j.foodhyd.2022.107757

Zhao, J., Bhandari, B., Gaiani, C., & Prakash, S. (2023). Fermentation of almond-based gel incorporated with double emulsion (W1/O/W2): A study on gel properties and effectiveness of double emulsion as a fat replacer. *Food Structure, 36*, Article 100322. https://doi.org/10.1016/j.foostr.2023.100322

Zhu, Y., Bhandari, B., & Prakash, S. (2018). Tribo-rheometry behaviour and gel strength of kappa-carrageenan and gelatin solutions at concentrations, pH and ionic conditions used in dairy products. *Food Hydrocolloids, 84*, 292–302. https://doi.org/10.1016/j.foodhyd.2018.06.016